HHS Public Access

Author manuscript

J Cell Physiol. Author manuscript; available in PMC 2022 June 01.

Published in final edited form as:

J Cell Physiol. 2021 June ; 236(6): 4360–4368. doi:10.1002/jcp.30153.

Lipopolysaccharide reduces USP13 stability through c-Jun N-terminal kinase activation in Kupffer cells

Fan Yu, **Yanhui Li**, **Qinmao Ye**, **Jiaxing Miao**, **Sarah J Taleb**, **Yutong Zhao**, **Jing Zhao***

Department of Physiology and Cell Biology, Dorothy M. Davis Heart and Lung Research Institute, The Ohio State University, Columbus, OH, USA

Abstract

Protein ubiquitination regulates protein stability, cellular localization, and enzyme activity. Deubiquitinases catalyze the removal of ubiquitin from target proteins and reverse ubiquitination. USP13, a deubiquitinase, has been shown to regulate a variety of cellular responses including inflammation; however, the molecular regulation of USP13 has not been demonstrated. In this study, we revealed that USP13 is degraded in response to lipopolysaccharide (LPS) in kupffer cells. USP13 levels are significantly decreased in inflamed organs, including liver tissues from septic mice. LPS reduces USP13 protein stability, not transcription, in kupffer cells. Furthermore, LPS increases USP13 polyubiquitination. Inhibition of proteasome, but not lysosome or immunoproteasome, attenuates LPS-induced USP13 degradation, suggesting USP13 degradation is mediated by the ubiquitin-proteasome system. A catalytically inactive form of USP13 exhibits similar degree of degradation compared to USP13 wild type, suggesting that USP13 degradation is not dependent on its activity. Furthermore, USP13 degradation is dependent on new protein synthesis. Inhibition of c-Jun N-terminal kinase (JNK) attenuates USP13 degradation, indicating that a JNK-dependent new protein synthesis is necessary for USP13 degradation. This study reveals a molecular mechanism of regulation of USP13 degradation in Kupffer cells in response to bacterial endotoxin.

Keywords

USP13; transcription; ubiquitination; proteasomal degradation; Kupffer cells

Introduction

Protein degradation is an essential process for maintenance of intracellular protein homeostasis (Balchin, Hayer-Hartl, & Hartl, 2016; Jana, 2012; Thompson & Bruick, 2012). Ubiquitination is the binding of an ubiquitin protein or ubiquitin chain to target proteins, resulting in protein degradation in either the proteasome or the lysosome (Berndsen &

*Address correspondence to: Jing Zhao, MD, PhD, Department of Physiology and Cell Biology, The Ohio State University, 333 10th Avenue, Graves Hall 2166D, Columbus, OH, United States, 43065, Tel: 614-685-0024, jing.zhao@osumc.edu.

Author contributions

F.Y., Y.L., Q.Y., J.M., S.J.T., and Y.Z. performed the experiments. F.Y. and Y.Z. wrote the draft, J.Z. guided project, and finalized the manuscript.

Conflict of Interest

The authors declare no competing financial interests.

Wolberger, 2014; Lee, Lee, & Rubinsztein, 2013; Zheng & Shabek, 2017). A series of enzyme reactions catalyze protein ubiquitination, which is reversible. Deubiquitination is the removal of ubiquitins or ubiquitin chains from target proteins (Hershko & Ciechanover, 1998; Mevissen & Komander, 2017; Varshavsky, 2017). Deubiquitinases catalyze this process and play critical roles in regulation of cellular responses, such as cell proliferation, cell death, differentiation, and cytokine release (Cai, Culley, Zhao, & Zhao, 2018; Clague, Urbe, & Komander, 2019; S. Li, Zhao, Shang, Kass, & Zhao, 2018). It is important to understand the molecular regulation of deubiquitinase activity, synthesis, and degradation. Regulation of deubiquitinases by post-translational modifications has been reported (Huang et al., 2011; Mevissen & Komander, 2017; Mialki, Zhao, Wei, Mallampalli, & Zhao, 2013). Phosphorylation of USP14 by AKT enhances its deubiquitinase activity (Huang et al., 2011; Xu et al., 2015). Deubiquitinase abundance is regulated by proteasomal degradation (Boutell, Canning, Orr, & Everett, 2005; Khoronenkova et al., 2012). Loss of activity may lead to deubiquitinase degradation. Inactive USP37 is ubiquitinated by E3 ubiquitin ligase APC^{CDH1} and degraded in the proteasome (Huang et al., 2011).

USP13, a deubiquitinase, is a type of cysteine protease. Multiple substrates have been identified as targets of USP13. USP13 targets and deubiquinates STING (stimulator of interferon genes), MCL1, PTEN, Myc, Sigirr, and others (Fang et al., 2017; L. Li et al., 2019; Liao et al., 2020; Sun et al., 2017; J. Zhang et al., 2013; S. Zhang et al., 2018); thus USP13 plays critical roles in regulation of various cellular responses including cell death and inflammation. There is limited information regarding molecular regulation of USP13 expression and activity. Our previous study has showed that USP13 levels are reduced in mouse lungs from murine models of acute lung injury (L. Li et al., 2019). Furthermore, LPS reduced *USP13* mRNA levels in Raw264.7 cells (L. Li et al., 2019). However, molecular mechanisms of *USP13* mRNA reduction have not been well revealed. Inhibition of NF-κB, JNK, and p38 had no effect on LPS-induced USP13 reduction (L. Li et al., 2019).

In this study, we found that USP13 levels are reduced in Kupffer cells in response to LPS. However, in contrast to USP13 mRNA changes in Raw264.7 cells, LPS reduces USP13 stability, but not mRNA levels, in Kupffer cells. Furthermore, we demonstrate that a new protein synthesis is necessary for USP13 degradation. It is possible that JNK plays a role in regulation of USP13 stability by upregulating synthesis of a new protein. This study is the first to demonstrate molecular regulation of USP13 stability and it will provide a new strategy to regulate biological functions of USP13 substrates.

Materials and Methods

Animal surgery procedure.

All procedures were approved by an institutional animal care and use committee (IACUC) at the Ohio State University Animal Resources Centers. Male C57BL/6 mice aged 8–10 weeks were housed under specific pathogen-free conditions at the Ohio State University. Cecal ligation and puncture (CLP) or sham operation was performed to induce sepsis. Briefly, mice were anesthetized by intraperitoneally injection of a mixture of ketamine and xylazine. Cecum was exposed, ligated at designated position, punctured with a 21-gauge needle, and gently squeezed to extrude a small amount of feces into the peritoneal cavity. Then the

wound was sutured, followed by liquid resuscitation with saline. Sham operation was performed with exposure of cecum but no ligation and puncture, and then cecum was placed back to the peritoneal cavity. At 4 or 24 h after the surgery, liver tissues were harvested. Murine model of acute lung injury was induced as previously described. Briefly, LPS (5mg/kg) or the same volume of PBS was injected into the trachea in each mouse. And then lung tissue samples were harvested after 24 h.

Cell culture and reagents.

HepG2 cells and Raw264.7 cells (mouse macrophage-like cell line) were purchased from American Type Cell Collection (ATCC, Rockville, MD, USA). The ImKC immortalized mouse Kupffer cells were purchased from EMD Millipore Corporation. HepG2, Raw264.7, and mouse Kupffer cells were cultured with complete medium composed of Dulbecco's Modified Medium (DMEM, from ATCC, Manassas, VA, USA) supplemented with 10% fetal bovine serum (FBS, Gemini Bio-Products, Calabasas, CA, USA) and 1% penicillin streptomycin (pen/strep, Gibco, Paisley, Scotland). MG-132 and leupeptin were from ENZO Life Sciences (Farmingdale, NY, USA). LPS, actinomycin D, cycloheximide, batimastat, SB203580, and anti-β-actin antibody were from Sigma Aldrich (St Louis, MO, USA). JNK inhibitor Ⅱ and Y27632 were from Calbiochem (San Diego, CA, USA). 5-azacytidine, BIX-02194, and ONX0914 were purchased from Cayman Chemical Company (Ann Arbor, MI, USA). Antibodies against Hsp90 and JNK, immobilized protein A&G beads and control IgG were from Santa Cruz Biotechnology (Santa Cruz, CA, USA). Anti-USP13 antibody was purchased from Proteintech (Chicago, IL, USA). Antibody against K48-linked ubiquitin was from Cell Signaling (Danvers, MA, USA). Anti-V5 antibody, mammalian expression plasmid pcDNA3.1/His-V5-topo and *Escherichia coli* TOP10 competent cells were from Life Technologies (Geithersburg, MD, USA). Horseradish perioxide-conjugated goat anti-rabbit and anti-mouse secondary antibodies were purchased from Bio-Rad (Hercules, CA, USA). GenJet™ and GenMute™ reagents were from SignaGen (Ijamsville, MD, USA).

Real-time reverse transcriptase-polymerase chain reaction.

Total RNA was extracted from cells by using the Total RNA Mini Kit (IBI Scientific, IA, USA) according to the manufacturer's instructions. The complementary (cDNA) was synthesized with 1 μg of total RNA using the iScript cDNA Synthesis Kit (Bio-Rad Laboratories, Hercules, CA, USA). Real-time RT-PCR was performed using the iQ SYBR Green Supermix kit (Bio-Rad Laboratories). Reaction mixture included cDNA template, forward and reverse primers, nuclease-free water, and the IQ Sybr Green supermix. The nucleotide sequences of specific primers are described below: *mUSP13* forward, AGTGCTCAGCTCAAAGTCCC, *mUsp13* reverse, AGTTGCACAAGGTTGTTGGC; *mIL-6* forward, AGCCAGAGTCCTTCAGAGAT, *mIL-6* reverse, GGAAATTGGGGTAGGAAGGACT; *mGapdh* forward, ACCCTTAAGAGGGATGCTGC, *mGapdh* reverse, TCACACCGACCTTCACCATTT. The mRNA level of each sample was normalized to that of *Gapdh* mRNA level.

Immunoblot analysis.

Proteins from liver tissues or cells were extracted by lysis buffer containing protease and phosphatase inhibitor (Thermo Fisher Scientific, Waltham, MA, USA). Cell lysates were

sonicated for 12 sec, followed by centrifugation at 4 °C at 10000 rpm for 5 min. Protein quantification was performed using the DC Protein Assay kit (Bio-Rad Laboratories, Hercules, CA, USA). Equal amounts of total protein (20 μg) were subjected to SDS-PAGE and transferred to nitrocellulose blotting membranes, then incubated with primary antibody, followed by the secondary antibody.

Plasmid and transfection.

The cDNA encoding human USP13 and mutants were inserted into pcDNA3.1-V5-His-Topo vector (Invitrogen, Carlsbad, CA, USA). After the cell density in 6-well plates or 100-mm dishes reached to 70%, plasmids were transfected into mouse Kupffer cells using GenJet™ reagent according to the manufacture's instruction.

In vivo ubiquitination assay.

Kupffer cells were treated with MG-132 for 3 h before they were collected. After washing with cold PBS, cells were harvested with PBS, followed by centrifugation at 1000 rpm for 5 min. Supernatant was removed, followed by addition of 1 μl of ubiquitin aldehyde, 1 μl of N-ethylmaleimide, and 60–80 μl of 2% SDS lysis buffer. After sonication, cell lysates were boiled at 100 °C for 10 min. The denatured samples were diluted with 600–800 μl of TBS. Equal quantities of protein (1 mg) from each sample were incubated with primary USP13 antibody for overnight at 4 °C to pull down USP13, then protein A&G beads were added for additional 2 h at 4 °C. The beads were precipitated by centrifugation at 2500 rpm for 2 min, and then rinsed with cold PBS three times. Precipitates were eluted by boiling in SDS sample buffer. Immunoblot analysis of the sample was performed with ubiquitin antibody.

Immunoblots quantification and Statistical analysis.

USP13 immunoblots were quantified with Image J and normalized to intensities of β-actin immunoblots. All results were subjected to statistical analysis using two-way ANOVA and, wherever appropriate, Student t test. Data are expressed as mean ± SD of triplicate samples from at least three independent experiments and p values <0.05 were considered statistically significant.

Results

USP13 levels are reduced in liver tissues in a cecal ligation and puncture (CLP)-induced sepsis model.

USP13, a deubiquitinase, regulates inflammatory responses through targeting IL-1R8/Sigirr (L. Li et al., 2019). We have shown that USP13 is reduced in lung tissues from a lipopolysaccharide (LPS)-induced acute lung injury model (L. Li et al., 2019). To further investigate molecular mechanisms of USP13 reduction in an inflammatory condition, we confirmed our published data and showed that intratracheal LPS challenge diminished USP13 protein levels in murine lungs (Fig. 1A and B). Further, we investigate the changes of USP13 in the liver from a CLP-induced sepsis model. As shown in Fig. 1C and D, USP13 levels in the liver were reduced in CLP-challenged mice, compared to that in sham mice. These results suggest that the anti-inflammatory USP13 is reduced in inflamed organs including lungs and liver.

USP13 levels are reduced in a macrophage like cell line (Raw264.7).

To investigate in which cell types that USP13 is reduced, we examined the USP13 levels in HepG2 and Raw264.7 (a macrophage cell like cell line). To mimic inflammatory condition, we treated HepG2 with LPS, IL-1β, and TNFα up to 48 h. As shown in Fig. 1E–G, and supplemental Fig. 1, neither LPS (low or high doses), IL-1β, nor TNFα altered USP13 levels. We found that LPS treatment of Raw264.7 cells diminished USP13 levels in both dose- and time-dependent manners (Fig. 1 H–K), consistent with our previous study.

LPS diminishes USP13 levels, but not *USP13* mRNA, in Kupffer cells.

Kupffer cells, resident macrophages in livers, play a critical role in liver inflammation, injury, and repair (Boltjes, Movita, Boonstra, & Woltman, 2014; Kolios, Valatas, & Kouroumalis, 2006). To investigate the molecular mechanisms by which LPS reduces USP13 levels in macrophages in the liver, we examined the effect of LPS on USP13 levels in Kupffer cells. The results were similar to the findings using Raw264.7 cells. LPS treatment starting from 10 ng/ml decreased USP13 levels after 24 h (Fig. 2A–D). Furthermore, changes of FBS concentration in culture media had no effect on LPS-reduction of USP13 in Kupffer cells. These data suggest that USP13 levels are reduced in Kupffer cells, but not hepatocytes. It is possible that hepatocytes and Kupffer cells express different levels of TLR4 and cytokine receptors. We have shown that LPS reduced *USP13* mRNA expression in Raw264.7 cells. Next, we investigated whether *USP13* mRNA changes in response to LPS in Kupffer cells. As shown in Fig. 3A, LPS treatment of Kupffer cells did not alter *USP13* mRNA expression. The western blotting further confirmed that LPS reduces USP13 protein levels without altering its transcription (Fig. 3B), suggesting that LPS may affect USP13 protein stability.

LPS induces USP13 degradation by the ubiquitin-proteasome system in Kupffer cells.

K48-linked polyubiquitination triggers protein degradation. To investigate whether LPS regulates USP13 degradation through ubiquitination, we examined the effect of LPS on USP13 ubiquitination. As shown in Fig. 4A, LPS increased USP13 lysine (K)48-linked polyubiquitination. Protein degradation is mediated in either the proteasome or the lysosome. To determine which pathway regulates USP13 degradation, we treated cells with proteasome inhibitors (MG-132 and bortezomib) or lysosome inhibitor (leupeptin) prior to LPS challenge. MG-132, but not leupeptin, attenuated LPS-induced USP13 degradation (Fig. 4B–D). Bortezomib treatment increased accumulation of USP13 (Fig. 4E), indicating that USP13 degradation is mediated by the ubiquitin-proteasome system. Immunoproteasome, a subgroup of proteasome, has been detected in inflammatory cells. Inhibition of the immunoproteasome by its specific inhibitor, ONX0914, did not alter USP13 degradation (Fig. 4E), suggesting that USP13 is degraded in the constitutive proteasome.

Catalytic activity of USP13 is not necessary for LPS-reduced USP13.

Inactivation of deubiquitinase has been shown to regulate its stability (Huang et al., 2011). To investigate whether catalytic activity of USP13 influences its stability, we generated a plasmid which expresses a catalytically inactive form of V5-tagged USP13 (USP13C345S-

V5). Cycloheximide is an inhibitor of protein synthesis and often used for examining protein half-life. As shown in Fig. 5A and B, USP13C345S delayed degradation, compared to USP13 wild type, while the differences did not reach statistical significance. Further, we investigated whether an inactive form of USP13 exhibits slightly longer half-life, compare to wild type, in the presence of LPS. Similar to endogenous USP13, ectopically expressed USP13-V5 was degraded in response to LPS, while USP13C345S-V5 exhibited an identical degradation pattern, compared to wild type (Fig. 5C, D). Thus, catalytic activity of USP13 is a minor factor for regulating its half-life, while it is not necessary for LPS-induced USP13 degradation.

LPS-induced synthesis of a new protein is required for USP13 reduction.

As shown above, LPS induced USP13 degradation in 24 h, but not in a shorter time exposure (4 and 8 h). Thus, we hypothesized that a new protein synthesis induced by LPS may target or promote USP13 for its ubiquitination. Actinomycin D is an inhibitor of mRNA synthesis. LPS-induced USP13 degradation was attenuated by actinomycin D (Fig. 6), suggesting a new protein induced by LPS regulates USP13 ubiquitination.

JNK activity is essential for USP13 degradation.

To investigate the molecular regulation of the unknown protein, which regulates USP13 ubiquitination and degradation, we examined several factors related to transcriptional regulation. Inhibitors of DNA methylation (5-azacytidine) and histone methylation (BIX-01294) had no effect on LPS-induced USP13 reduction (Fig. 7A–C). Furthermore, among the inhibitors of matrix metalloproteinases (MMPs), ROCK, p38 MAPK, and JNK, only JNK inhibitor II attenuated USP13 degradation (Fig. 7D). The effect of JNK inhibitor II on LPS-induced USP13 degradation was confirmed by an experiment using increasing doses of the inhibitor (Fig. 7E). JNKs have been well known as downstream signal molecules and to regulate LPS-induced gene expression and protein synthesis. This data suggests that LPS induces synthesis of a USP13 degrading protein through activation of JNK in Kupffer cells.

Discussion

USP13 plays roles in various cellular responses by targeting multiple substrate proteins (Fang et al., 2017; L. Li et al., 2019; Liao et al., 2020; Sun et al., 2017; J. Zhang et al., 2013; S. Zhang et al., 2018). We have focused on investigating role of USP13 in inflammatory responses. Our previous study suggests that USP13 exhibits an anti-inflammatory property by stabilizing an anti-inflammatory receptor, IL-1R8/Sigirr (L. Li et al., 2019). Inhibition of overexpression of USP13 regulates LPS-induced inflammatory responses (L. Li et al., 2019). In the study, we also revealed that USP13 expression is reduced in inflamed lungs and LPS-challenged Raw264.7 cells. In the current study, we confirmed the findings and further discovered that in addition to lung tissues, USP13 is diminished in liver tissue from mouse under septic shock. Notably, Kupffer cells, but not hepatocytes, exhibit a reduction of USP13 in response to LPS challenge. Both Kupffer cells and Raw264.7 cells express Toll-like receptor 4 (TLR4) and are sensitive to LPS (El Kasmi et al., 2012; Fisher et al., 2013; Schmitz, Mages, Heit, Lang, & Wagner, 2004). We revealed that LPS reduces USP13 protein levels in both cell types, while *USP13* mRNA is reduced in Raw264.7 cells, but not

in Kupffer cells. In Raw264.7 cells, LPS-reduced USP13 protein levels is by diminishing its transcription, while in Kupffer cells, USP13 reduction is due to increased ubiquitination and proteasomal degradation. The different phenotypes in these two cell types are possibly due to the fact that Kupffer cells are liver tissue specific macrophages. Kupffer cells have been shown to express unique gene expression patterns compared to peripheral macropaghes, such as relatively low expression of tmed1, tollip, and IRAK-M in Kupffer cells (Movita et al., 2012). It is possible that these different gene profiles affect regulation of USP13 degradation in Kupffer cells and Raw264.7 cells.

Deubiquitinase stability has not been well demonstrated. Here, we report that USP13 degradation is mediated by the ubiquitin-proteasome system. LPS-induced K48-linked polyubiquitination of USP13 is responsible for its proteasomal degradation. Changes in catalytic activity of deubiquitinases may determine their protein stability (Huang et al., 2011; Mevissen & Komander, 2017). Loss of deubiquitinase activity may increase its degradation. It is possible that deubiquitinases exhibit self-catalytic activity and prevent themselves from ubiquitination and degradation. We generated a catalytically inactive form of USP13 and revealed that enzyme activity in wild type USP13 slightly increases its half-life, compared to inactive form. However, the differences were not observed in response to LPS challenge, suggesting that an E3 ubiquitin ligase targets USP13 independently of USP13 activity.

We found that short time exposure of LPS did not trigger USP13 degradation, suggesting that an immediate LPS signaling through TLR4 does not contribute to USP13 ubiquitination and degradation. Furthermore, we showed that JNK-mediated synthesis of a new protein is necessary for USP13 degradation. The unidentified protein may be an ubiquitin E3 ligase or other mediator that promotes USP13 proteasomal degradation. We have not determined whether this newly synthesized protein is an E3 ubiquitin ligase or not. We have found that LPS increased Smurf1 and WWP1 expression in Kupffer cells (data not shown). None of these E3 ubiquitin ligases are responsible for USP13 degradation (data not shown). Inhibition of JNK had no effect on LPS reduction of USP13 in Raw264.7 cells, while JNK inhibitor attenuates USP13 degradation in Kupffer cells. This suggests that molecular regulation of USP13 is different in these two cell types. From the time points of LPS' effect, we hypothesized that activation of JNK by LPS does not directly affect USP13 ubiquitination. JNK was not associated with USP13 in both 4 and 16 h after LPS treatment (supplemental Fig. 2). Which JNK isoform is involved in USP13 degradation has not been revealed. The upstream signal pathways of JNK, such as TRAF and MEKK1, may also regulate USP13 degradation. C-Jun is a substrate JNK. We will further identify the JNK/c-Jun-regulated newly synthesized proteins under LPS challenge in future studies.

The role of USP13 in macrophages including Kupffer cells have not been demonstrated. We have shown that USP13 regulates Sigirr stability, thus we hypothesize that USP13 may play an anti-inflammatory role in Kupffer cells. This study indicates that understanding of USP13 degradation may reveal new molecular mechanisms in inflammatory responses. The effect of USP13 on anti-inflammatory receptor Sigirr's or other anti-inflammatory mediators' stability in Kupffer cells needs to be determined in future studies. The roles of USP13 and

the newly synthesized protein in liver inflammation, injury, and repair will be the future focuses.

Supplementary Material

Refer to Web version on PubMed Central for supplementary material.

Acknowledgement

This work was supported by grants from National Institutes of Health (R01HL131665, HL112791, HL136294 to Y.Z., R01 GM115389, R01HL151513 to J.Z.). All the authors have read the journal's authorship agreement and that the manuscript has been reviewed by and approved by all named authors.

Abbreviations:

LPS	lipopolysaccharide
JNK	c-Jun N-terminal kinase
STING	stimulator of interferon genes
CLP	cecal ligation and puncture
MMP	matrix metalloproteinase
TLR4	toll like receptor 4

References

Balchin D, Hayer-Hartl M, & Hartl FU (2016). In vivo aspects of protein folding and quality control. Science, 353(6294), aac4354. doi:10.1126/science.aac4354 [PubMed: 27365453]

Berndsen CE, & Wolberger C (2014). New insights into ubiquitin E3 ligase mechanism. Nat Struct Mol Biol, 21(4), 301–307. doi:10.1038/nsmb.2780 [PubMed: 24699078]

Boltjes A, Movita D, Boonstra A, & Woltman AM (2014). The role of Kupffer cells in hepatitis B and hepatitis C virus infections. J Hepatol, 61(3), 660–671. doi:10.1016/j.jhep.2014.04.026 [PubMed: 24798624]

Boutell C, Canning M, Orr A, & Everett RD (2005). Reciprocal activities between herpes simplex virus type 1 regulatory protein ICP0, a ubiquitin E3 ligase, and ubiquitin-specific protease USP7. J Virol, 79(19), 12342–12354. doi:10.1128/JVI.79.19.12342-12354.2005 [PubMed: 16160161]

Cai J, Culley MK, Zhao Y, & Zhao J (2018). The role of ubiquitination and deubiquitination in the regulation of cell junctions. Protein Cell, 9(9), 754–769. doi:10.1007/s13238-017-0486-3 [PubMed: 29080116]

Clague MJ, Urbe S, & Komander D (2019). Breaking the chains: deubiquitylating enzyme specificity begets function. Nat Rev Mol Cell Biol, 20(6), 338–352. doi:10.1038/s41580-019-0099-1 [PubMed: 30733604]

El Kasmi KC, Anderson AL, Devereaux MW, Fillon SA, Harris JK, Lovell MA, … Sokol RJ (2012). Toll-like receptor 4-dependent Kupffer cell activation and liver injury in a novel mouse model of parenteral nutrition and intestinal injury. Hepatology, 55(5), 1518–1528. doi:10.1002/hep.25500 [PubMed: 22120983]

Fang X, Zhou W, Wu Q, Huang Z, Shi Y, Yang K, … Bao S (2017). Deubiquitinase USP13 maintains glioblastoma stem cells by antagonizing FBXL14-mediated Myc ubiquitination. J Exp Med, 214(1), 245–267. doi:10.1084/jem.20151673 [PubMed: 27923907]

Fisher JE, McKenzie TJ, Lillegard JB, Yu Y, Juskewitch JE, Nedredal GI, … Nyberg SL (2013). Role of Kupffer cells and toll-like receptor 4 in acetaminophen-induced acute liver failure. J Surg Res, 180(1), 147–155. doi:10.1016/j.jss.2012.11.051 [PubMed: 23260383]

Hershko A, & Ciechanover A (1998). The ubiquitin system. Annu Rev Biochem, 67, 425–479. doi:10.1146/annurev.biochem.67.1.425 [PubMed: 9759494]

Huang X, Summers MK, Pham V, Lill JR, Liu J, Lee G, … Dixit VM (2011). Deubiquitinase USP37 is activated by CDK2 to antagonize APC(CDH1) and promote S phase entry. Mol Cell, 42(4), 511–523. doi:10.1016/j.molcel.2011.03.027 [PubMed: 21596315]

Jana NR (2012). Protein homeostasis and aging: role of ubiquitin protein ligases. Neurochem Int, 60(5), 443–447. doi:10.1016/j.neuint.2012.02.009 [PubMed: 22353631]

Khoronenkova SV, Dianova II, Ternette N, Kessler BM, Parsons JL, & Dianov GL (2012). ATM-dependent downregulation of USP7/HAUSP by PPM1G activates p53 response to DNA damage. Mol Cell, 45(6), 801–813. doi:10.1016/j.molcel.2012.01.021 [PubMed: 22361354]

Kolios G, Valatas V, & Kouroumalis E (2006). Role of Kupffer cells in the pathogenesis of liver disease. World J Gastroenterol, 12(46), 7413–7420. doi:10.3748/wjg.v12.i46.7413 [PubMed: 17167827]

Lee MJ, Lee JH, & Rubinsztein DC (2013). Tau degradation: the ubiquitin-proteasome system versus the autophagy-lysosome system. Prog Neurobiol, 105, 49–59. doi:10.1016/j.pneurobio.2013.03.001 [PubMed: 23528736]

Li L, Wei J, Li S, Jacko AM, Weathington NM, Mallampalli RK, … Zhao Y (2019). The deubiquitinase USP13 stabilizes the anti-inflammatory receptor IL-1R8/Sigirr to suppress lung inflammation. EBioMedicine, 45, 553–562. doi:10.1016/j.ebiom.2019.06.011 [PubMed: 31204278]

Li S, Zhao J, Shang D, Kass DJ, & Zhao Y (2018). Ubiquitination and deubiquitination emerge as players in idiopathic pulmonary fibrosis pathogenesis and treatment. JCI Insight, 3(10). doi:10.1172/jci.insight.120362

Liao X, Li Y, Liu J, Zhang Y, Tan J, Kass DJ, … Zhao Y (2020). Deubiquitinase USP13 promotes extracellular matrix expression by stabilizing Smad4 in lung fibroblast cells. Transl Res. doi:10.1016/j.trsl.2020.05.004

Mevissen TET, & Komander D (2017). Mechanisms of Deubiquitinase Specificity and Regulation. Annu Rev Biochem, 86, 159–192. doi:10.1146/annurev-biochem-061516-044916 [PubMed: 28498721]

Mialki RK, Zhao J, Wei J, Mallampalli DF, & Zhao Y (2013). Overexpression of USP14 protease reduces I-kappaB protein levels and increases cytokine release in lung epithelial cells. J Biol Chem, 288(22), 15437–15441. doi:10.1074/jbc.C112.446682 [PubMed: 23615914]

Movita D, Kreefft K, Biesta P, van Oudenaren A, Leenen PJ, Janssen HL, & Boonstra A (2012). Kupffer cells express a unique combination of phenotypic and functional characteristics compared with splenic and peritoneal macrophages. J Leukoc Biol, 92(4), 723–733. doi:10.1189/jlb.1111566 [PubMed: 22685319]

Schmitz F, Mages J, Heit A, Lang R, & Wagner H (2004). Transcriptional activation induced in macrophages by Toll-like receptor (TLR) ligands: from expression profiling to a model of TLR signaling. Eur J Immunol, 34(10), 2863–2873. doi:10.1002/eji.200425228 [PubMed: 15368303]

Sun H, Zhang Q, Jing YY, Zhang M, Wang HY, Cai Z, … Zhong B (2017). USP13 negatively regulates antiviral responses by deubiquitinating STING. Nat Commun, 8, 15534. doi:10.1038/ncomms15534 [PubMed: 28534493]

Thompson JW, & Bruick RK (2012). Protein degradation and iron homeostasis. Biochim Biophys Acta, 1823(9), 1484–1490. doi:10.1016/j.bbamcr.2012.02.003 [PubMed: 22349011]

Varshavsky A (2017). The Ubiquitin System, Autophagy, and Regulated Protein Degradation. Annu Rev Biochem, 86, 123–128. doi:10.1146/annurev-biochem-061516-044859 [PubMed: 28654326]

Xu D, Shan B, Lee BH, Zhu K, Zhang T, Sun H, … Yuan J (2015). Phosphorylation and activation of ubiquitin-specific protease-14 by Akt regulates the ubiquitin-proteasome system. Elife, 4, e10510. doi:10.7554/eLife.10510 [PubMed: 26523394]

Zhang J, Zhang P, Wei Y, Piao HL, Wang W, Maddika S, … Ma L (2013). Deubiquitylation and stabilization of PTEN by USP13. Nat Cell Biol, 15(12), 1486–1494. doi:10.1038/ncb2874 [PubMed: 24270891]

Zhang S, Zhang M, Jing Y, Yin X, Ma P, Zhang Z, … Zhuang G (2018). Deubiquitinase USP13 dictates MCL1 stability and sensitivity to BH3 mimetic inhibitors. Nat Commun, 9(1), 215. doi:10.1038/s41467-017-02693-9 [PubMed: 29335437]

Zheng N, & Shabek N (2017). Ubiquitin Ligases: Structure, Function, and Regulation. Annu Rev Biochem, 86, 129–157. doi:10.1146/annurev-biochem-060815-014922 [PubMed: 28375744]

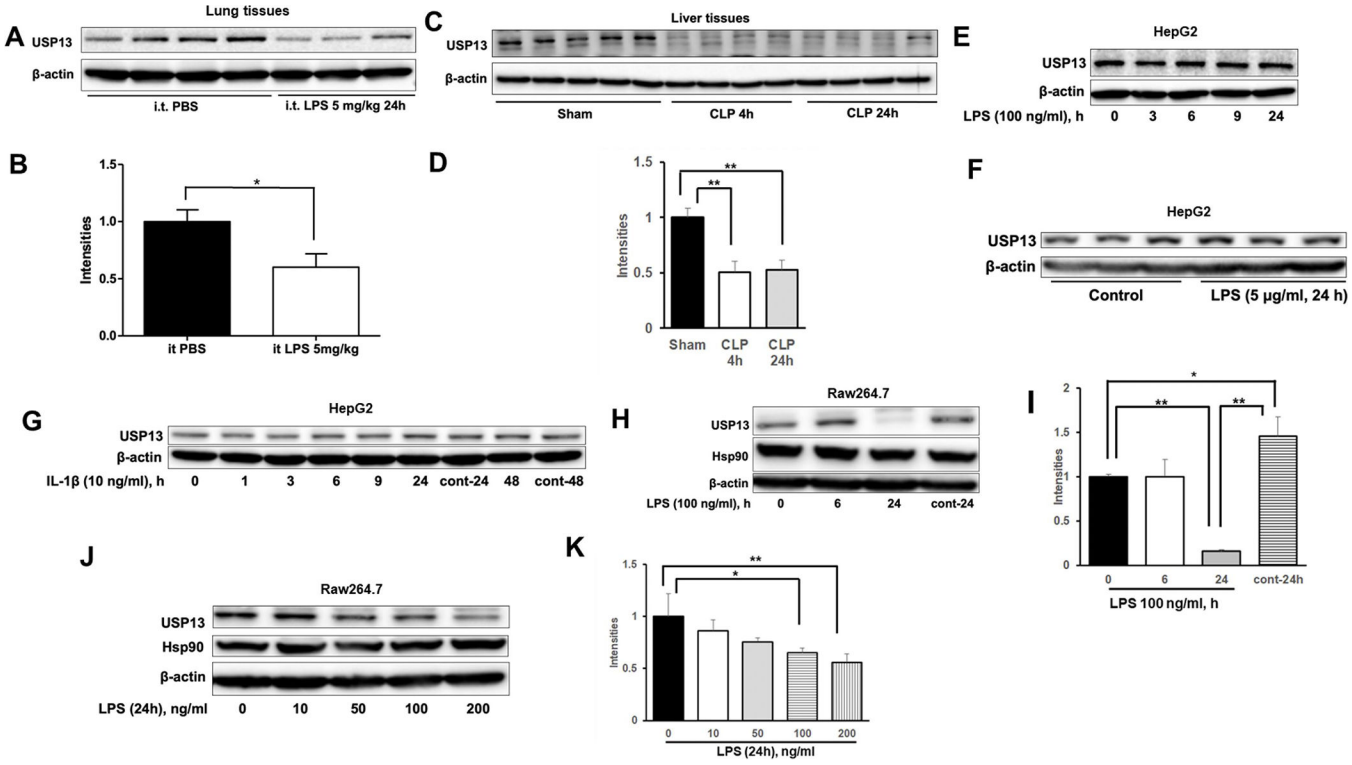

Figure 1. USP13 levels are reduced in liver tissue from a CLP-induced murine model of sepsis and in Raw264.7 cells in response to LPS.

A. Immunoblotting analysis of lung tissue lysates from intratracheal PBS and LPS-challenged mice with antibodies against USP13 and β-actin. **B.** USP13 immunoblots from **A** were quantified with Image J and normalized to intensities of β-actin immunoblots. *p<0.05, n=3–4. **C.** Immunoblotting analysis of liver tissue lysates from sham and CLP-challenged mice with antibodies against USP13 and β-actin. **D.** USP13 immunoblots from **C** were quantified with Image J and normalized to intensities of β-actin immunoblots. *p<0.05, n=4–5. **E.** Immunoblotting analysis of cell lysates from HepG2 treated with lower concentration of LPS (100 ng/ml, 0–24 h) with antibodies against USP13 and β-actin. **F.** Immunoblotting analysis of cell lysates from HepG2 treated with higher concentration of LPS (5 μg/ml, 24 h) with antibodies against USP13 and β-actin. **G.** Immunoblotting analysis of cell lysates from HepG2 treated with IL- 1β (10 ng/ml, 0–48 h) with antibodies against USP13 and β-actin. **H.** Immunoblotting analysis of cell lysates from Raw264.7 treated with LPS (100 ng/ml, 0–24 h) with antibodies against USP13, Hsp90, and β-actin. **I.** USP13 immunoblots from **H** were quantified with Image J and normalized to intensities of β-actin immunoblots. *p<0.05, **p<0.01, n=3. **J.** Immunoblotting analysis of cell lysates from Raw264.7 treated with LPS (0–200 ng/ml, 24 h) with antibodies against USP13, Hsp90, and β-actin. **K.** USP13 immunoblots from **H** were quantified with Image J and normalized to intensities of β-actin immunoblots. *p<0.05, **p<0.01, n=3. All the images (**E-J**) are representative from three independent experiments.

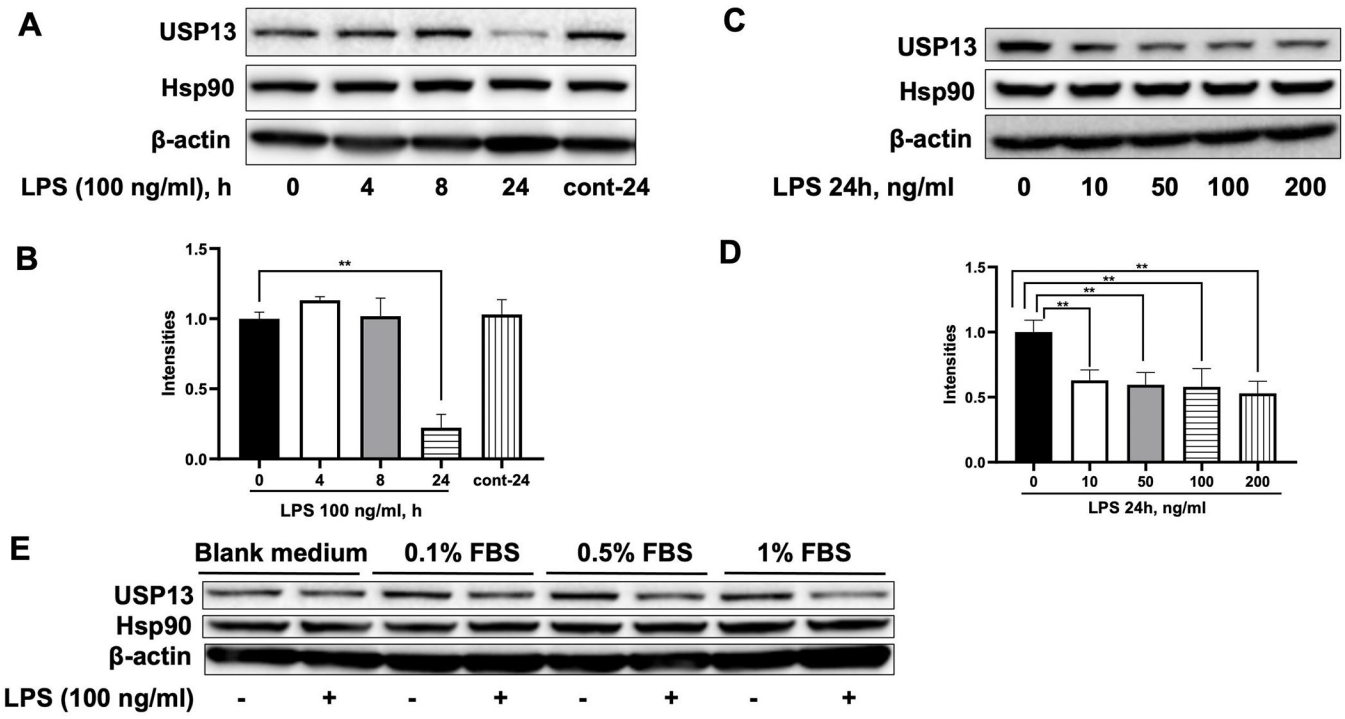

Figure 2. LPS reduces USP13 levels in Kupffer cells.

A. Immunoblotting analysis of cell lysates from Kupffer cells treated with LPS (100 ng/ml, 0–24 h) with antibodies against USP13, Hsp90, and β-actin. **B.** USP13 immunoblots from **A** were quantified with Image J and normalized to intensities of β-actin immunoblots. **p<0.01, n=3. **C.** Immunoblotting analysis of cell lysates from Kupffer cells treated with LPS (0–200 ng/ml) for 24 h with antibodies against USP13, Hsp90, and β-actin. **D.** USP13 immunoblots from **C** were quantified with Image J and normalized to intensities of β-actin immunoblots. **p<0.01, n=3. **E.** Immunoblotting analysis of cell lysates from Kupffer cells in different concentration of FBS culture media treated with LPS (100 ng/ml, 24 h) with antibodies against USP13, Hsp90, and β-actin. All the images are representative from three independent experiments.

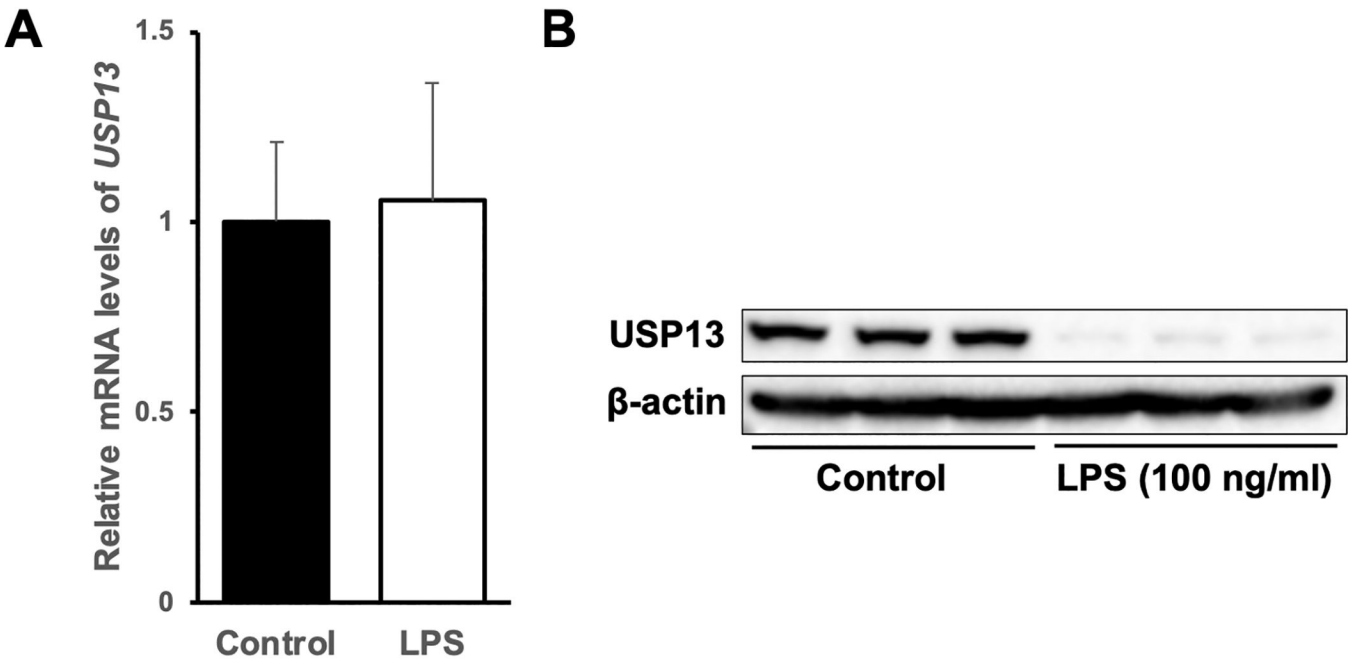

Figure 3. USP13 mRNA levels remains unchanged in response to LPS exposure.

Kupffer cells were treated with LPS (100 ng/ml, 24 h), and then total RNA was extracted for realtime PCR. **A.** USP13 mRNA levels were examined by realtime PCR. **p<0.01, n=3. **B.** Cell lysates were analyzed by immunoblotting with antibodies against USP13 and β-actin.

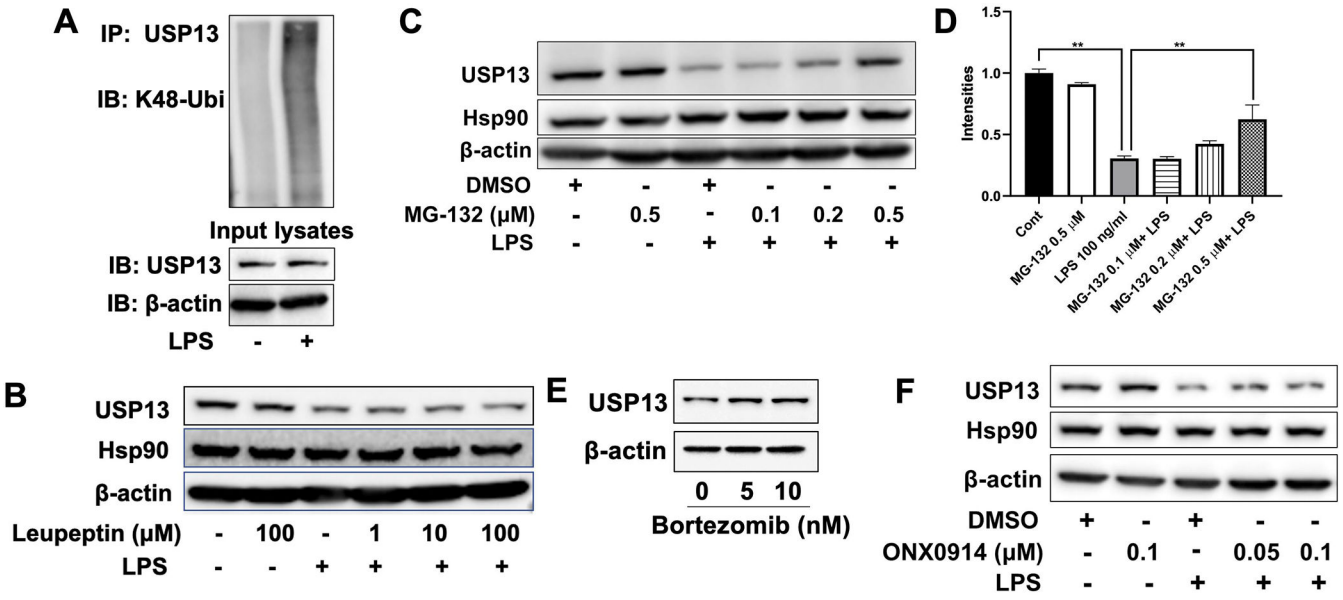

Figure 4. USP13 degradation by LPS is mediated by the ubiquitin-proteasome system.

A. Denatured cell lysates from LPS (100 ng/ml, 16 h)-treated Kupffer cells were subjected to immunoprecipitation with a USP13 antibody, followed by immunoblotting with K48-linked ubiquitin antibodies. Input lysates were analyzed by immunoblotting with USP13 and β-actin antibodies. **B.** Immunoblotting analysis of cell lysates from Kupffer cells treated with LPS (100 ng/ml, 24 h) with or without leupeptin with antibodies against USP13, Hsp90, and β-actin. **C.** Immunoblotting analysis of cell lysates from Kupffer cells treated with LPS (100 ng/ml, 24 h) with or without MG-132 with antibodies against USP13, Hsp90, and β-actin. **D.** USP13 immunoblots from **C** were quantified with Image J and normalized to intensities of β-actin immunoblots. **p<0.01, n=3. **E.** Immunoblotting analysis of cell lysates from Kupffer cells treated with bortezomib for 24 h. **F.** Immunoblotting analysis of cell lysates from Kupffer cells treated with LPS (100 ng/ml, 24 h) with or without ONX0914 with antibodies against USP13, Hsp90, and β-actin. All the images are representative from three independent experiments.

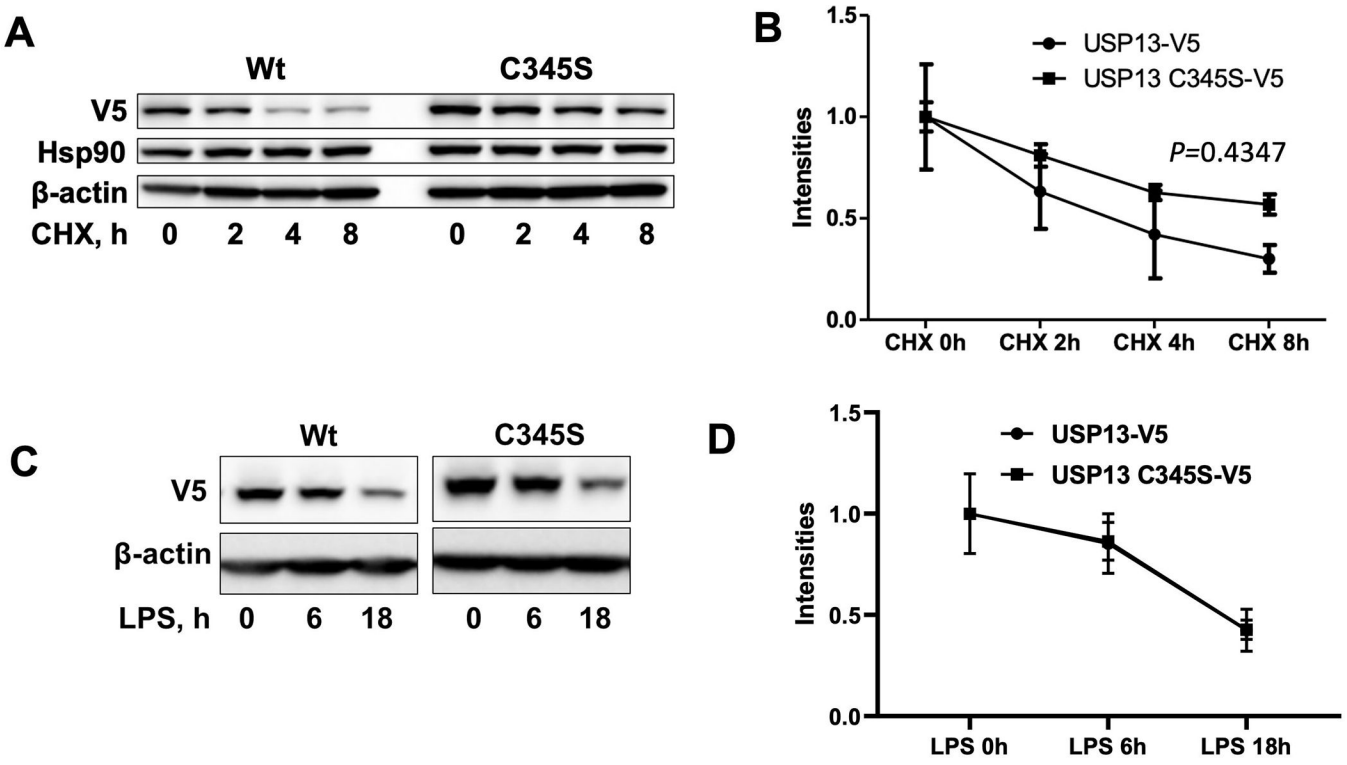

Figure 5. Catalytic activity of USP13 is not involved in LPS-induced USP13 degradation.

A. Kupffer cells were transfected with V5-tagged USP13 wild type (Wt) or USP13C345S plasmid for 48 h, and then cells were treated with CHX for 0–8 h. Immunoblotting analysis of cell lysates with antibodies against V5, Hsp90, and β-actin. **B.** USP13 immunoblots from **A** were quantified with Image J and normalized to intensities of β-actin immunoblots. **C.** Kupffer cells were transfected with V5-tagged USP13 wild type (Wt) or USP13C345S plasmid for 48 h, and then cells were treated with LPS (100 ng/ml) for 0–18 h. Immunoblotting analysis of cell lysates with antibodies against V5 and β-actin. **D.** USP13 immunoblots from **C** were quantified with Image J and normalized to intensities of β-actin immunoblots. All the images are representative from three independent experiments.

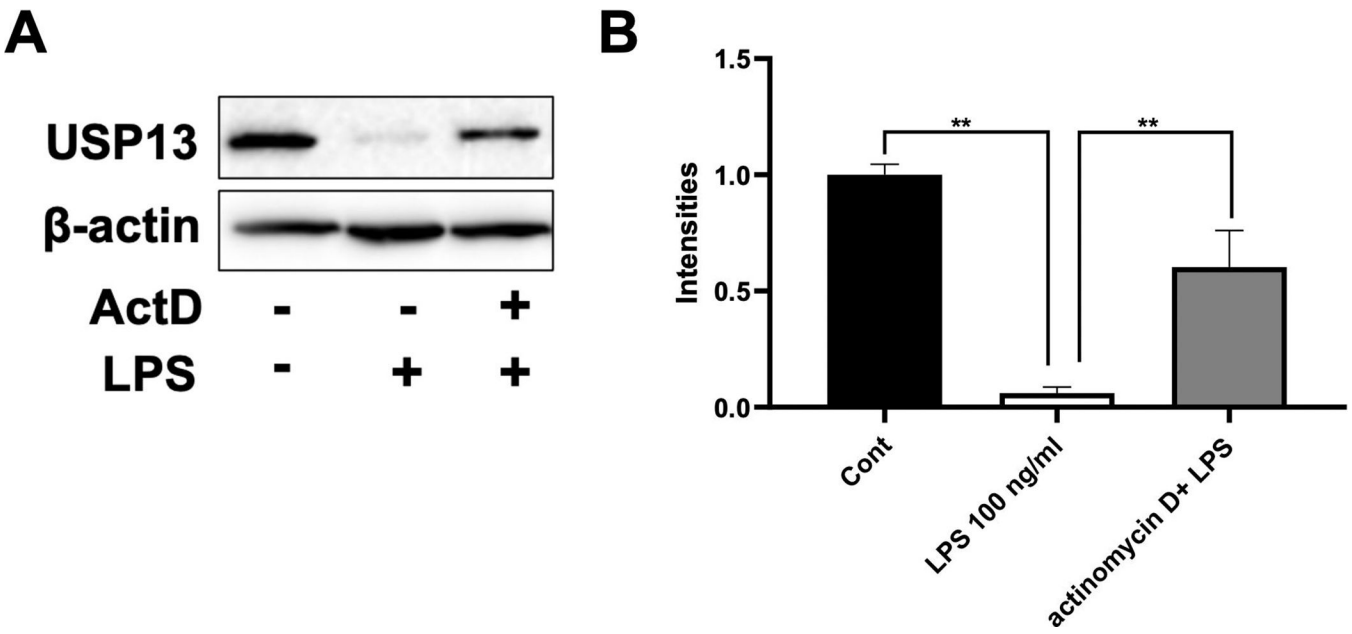

Figure 6. Actinomycin D attenuates LPS-induced USP13 degradation.

A. Immunoblotting analysis of cell lysates from Kupffer cells treated with LPS (100 ng/ml, 24 h) with or without actinomycin D (ActD) with antibodies against USP13 and β-actin. **B.** USP13 immunoblots from **A** were quantified with Image J and normalized to intensities of β-actin immunoblots. **p<0.01, n=3. All the images are representative from three independent experiments.

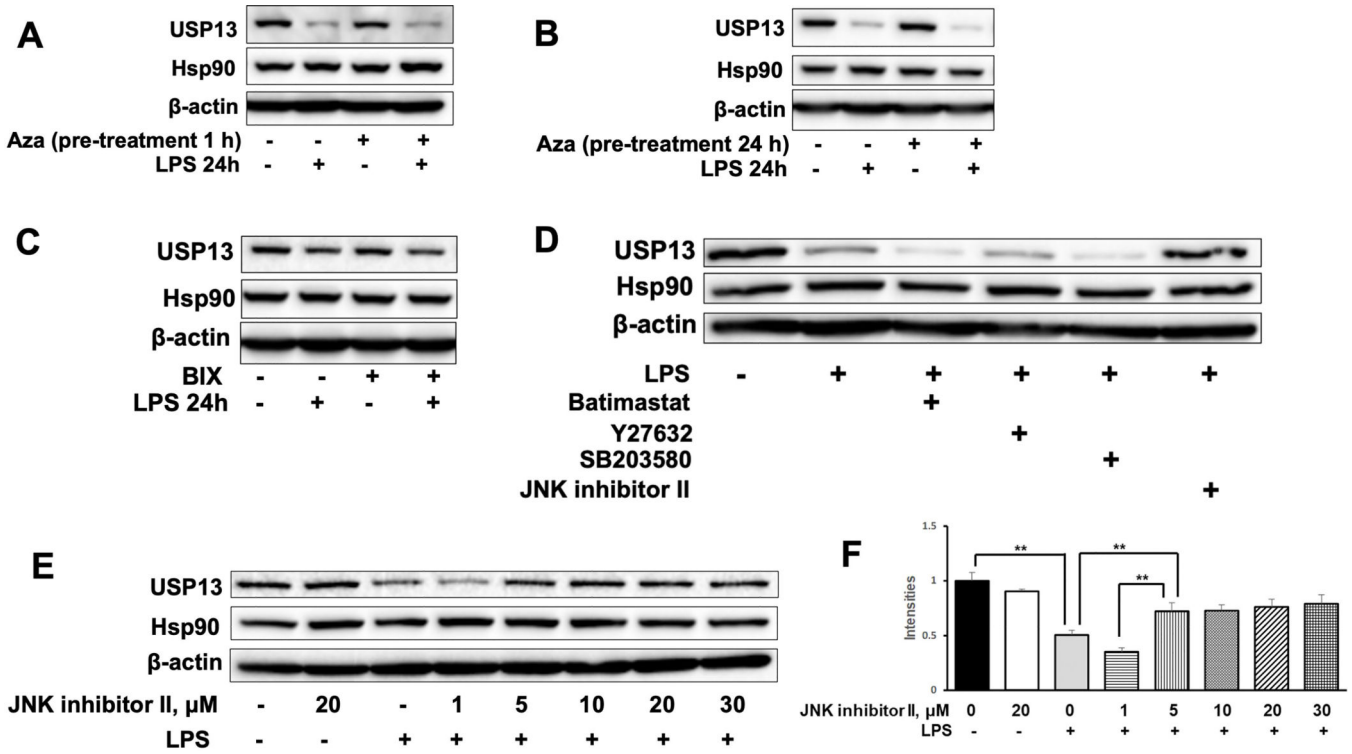

Figure 7. JNK inhibitor attenuates LPS-induced USP13 degradation.

A. Immunoblotting analysis of cell lysates from Kupffer cells treated with LPS (100 ng/ml, 24 h) with or without 5-azacytidine (Aza, pretreatment 1 h) with antibodies against USP13, Hsp90, and β-actin. **B.** Immunoblotting analysis of cell lysates from Kupffer cells treated with LPS (100 ng/ml, 24 h) with or without 5-azacytidine (Aza, pretreatment 24 h) with antibodies against USP13, Hsp90, and β-actin. **C.** Immunoblotting analysis of cell lysates from Kupffer cells treated with LPS (100 ng/ml, 24 h) with or without BIX-01294 (BIX) with antibodies against USP13, Hsp90, and β-actin. **D.** Immunoblotting analysis of cell lysates from Kupffer cells treated with LPS (100 ng/ml, 24 h) with or without indicated inhibitors with antibodies against USP13, Hsp90, and β-actin. **E.** Immunoblotting analysis of cell lysates from Kupffer cells treated with LPS (100 ng/ml, 24 h) with or without JNK inhibitor II (0–30 μM) with antibodies against USP13, Hsp90, and β-actin. **F.** USP13 immunoblots from **E** were quantified with Image J and normalized to intensities of β-actin immunoblots. **p<0.01, n=3. All the images are representative from three independent experiments.